第7卷 第3期
2014年6月

中国光学
Chinese Optics

Vol. 7 No. 3
Jun. 2014

文章编号 2095-1531(2014)03-0411-10

Simulation on the law of wave-front shaping with stochastic parallel gradient descent algorithm for adaptive optics

WANG Wei-bing*, WANG Ting-feng, GUO Jin

(*State Key Laboratory of Laser Interaction with Matter, Changchun Institute of Optics, Fine Mechanics and Physics, Chinese Academy of Sciences, Changchun* 130033, *China*)

* *Corresponding author*, *E-mail*: *wangweibing*10@126.*com*

Abstract: Firstly, we introduce the principle of wave-front shaping with stochastic parallel gradient descent (SPGD) algorithm based on Zernike mode for adaptive optics in atmospheric turbulence, and achieve brief expression about Strehl ratio that makes convergence rate of SPGD algorithm be accelerated obviously. Then we construct wave-front shaping system with SPGD algorithm of specific parameters, and mainly make detailed simulations on the laws of convergence rate, shaping capability and shaping effect about distortion wave-front, Zernike order and actuator number of deformable mirror. The qualitative results show that three change laws are similar, and quantitative expressions of shaping capability and shaping effect are achieved by the least square method. And it can be found from discussion that it's better to select 37-unit deformable mirror to shape 3 ~ 27(25) order Zernike aberrations of distortion wave-front at the conditions of some shaping effect considering the nature of real-time and simplification of system.

Key words: wave-front shaping for adaptive optics; stochastic parallel gradient descent algorithm; convergence rate; shaping capability; shaping effect

自适应光学随机并行梯度下降算法波前整形规律仿真

王卫兵*,王挺峰,郭 劲

(中国科学院 长春光学精密机械与物理研究所
激光与物质相互作用国家重点实验室,吉林 长春 130033)

摘要:本文首先介绍了基于 Zernike 模式的 SPGD 算法对大气湍流畸变波前的整形原理,通过推导得到了关于性能指标的简明表达式,使 SPGD 算法收敛速率得到明显提升。然后建立了自适应光学随机并行梯度下降算法波前整形系统模型,主要对 SPGD 算法收敛速率、整形能力和整形效果随波前畸变量和变形镜模型的变化规律作了较为详细的仿真研

收稿日期:2013-12-16;**修订日期**:2014-02-13

基金项目:吉林省重大科技攻关专项资助项目(No. 20120615)

究,整体定性结果表明:三者的变化规律有一定的相似性,同时利用最小二乘法得到了关于整形能力和整形效果变化规律的定量表达式,若从自适应光学波前整形系统的实时性和简单性考虑,在保证一定整形效果的情况下,选择37单元变形镜对畸变波前的3~27(25)阶Zernike像差进行整形即可。

关 键 词:自适应光学波前整形;随机并行梯度下降算法;收敛速率;整形能力;整形效果

中图分类号:TP301;TN241 **文献标识码**:A doi:10.3788/CO.20140703.0411

1 Introduction

How to shape distortion wave-front produced by atmospheric turbulence is a study focus in optical communications and optical imaging. Recently, many institutions have been doing many researches on distortion wave-front shaping by controlling deformable mirror with stochastic parallel gradient descent (SPGD) algorithm. This adaptive optics system without wave-front sensor can cut down the cost of system and solve the problem that wave-front can't be detected because of light spot scintillation[1].

In 1997, M. A. Vorontsov et. al successfully used SPGD algorithm in adaptive phase-distortion correction[2], and then used SPGD algorithm in laser focusing, laser communications, APPLE system[3] and astronomy imaging. In 2000, M. A. Vorontsov et. al investigated convergence rate of SPGD algorithm by controlling different elements liquid-crystal phase modulator[4]. In 2009, Yang Huizhen *et al*. made many simulations for shaping distortion wave-front described by 3 ~ 104 order Zernike aberrations by controlling 61-unit deformable mirror with SPGD algorithm from convergence rate and image quality of SPGD algorithm, and achieved good shaping effects[5]. It can be found from many relative papers[1-8] involved with SPGD algorithm that no one has investigated in detail and systematically the change laws of convergence rate, shaping capability and shaping effect of SPGD algorithm. In this paper we focus on the above problems.

We use 6 frames of different distortion degree of initial wave-front described by 3 ~ 119(117) order Zernike aberrations with Roddier method[9] as shaping objects and 6 kinds of different unit deformable mirror as shaping device, and construct wave-front shaping system with SPGD algorithm for adaptive optics by selecting appropriate algorithm parameters, and make detailed simulations for the law of adaptive optics for wave-front shaping with SPGD algorithm in atmospheric turbulence.

2 Principle of wave-front shaping with SPGD algorithm based on Zernike mode for adaptive optics in atmospheric turbulence

2.1 Wave-front shaping theory based on Zernike mode in atmospheric turbulence

The degree of atmospheric turbulence can be measured by atmospheric coherence length r_0, and produced distortion wave-front can be analyzed by Zernike mode method. Results achieved by Noll show that Zernike mode is not independent in statistic. And Roddier solved this problem with Karhunen-Loeve function by metric computations, and all wave-front phase can be fitted by Zernike polynomials. Distortion wave-front described by 3 ~ M + 3 (total: M) order Zernike aberrations (not including Zernike tilt aberrations) with Roddier method[9] is expressed as

$$\varphi(x,y) = \sum_{i=3}^{M+3} a_i Z_i(x,y) + \varepsilon \approx \sum_{i=1}^{M} a_i Z_i(x,y) , \quad (1)$$

where ε is fit residua neglected, $Z_i(x,y)$ is i-th

Zernike polynomial and a_i is the corresponding coefficient. Expression (1) shows clearly that M, a_i and $Z_i(x,y)$ all influence distortion degree of wave-front, and number of a_i and $Z_i(x,y)$ is M. When M is fixed, $Z_i(x,y)$ is also fixed. So distortion degree of wave-front mainly depends on M and a_i. By this way can we obtain different wave-front with different M and a_i. Surface function (or phase compensation) of N-unit deformable mirror[5,7] is expressed as

$$w(x,y) = \sum_{j=1}^{N} v_j S_j(x,y) + \varepsilon' , \quad (2)$$

$$S_j(x,y) = \exp\left\{\ln\omega \cdot \left[\frac{\sqrt{(x-x_j)^2 + (y-y_j)^2}}{d}\right]^{\alpha}\right\} , \quad (3)$$

where ε' is fit residua neglected, ω is the coupling value between actuators, d is the distance between actuators and α is the Gaussian index. j is j-th actuator of deformable mirror, $S_j(x,y)$ is response function of the j-th actuator, (x_j,y_j) is location of the j-th actuator and v_j is control voltage of the j-th actuator.

If using the same Zernike polynomials $Z_i(x,y)$ to fit $S_j(x,y)$, $S_j(x,y)$ can be expressed as

$$S_j(x,y) = \sum_{i=1}^{M} b_{ij} Z_i(x,y) + \varepsilon'' , \quad (4)$$

$$b_{ij} = \iint_S Z_i(x,y) S_j(x,y)\,\mathrm{d}x\mathrm{d}y , \quad (5)$$

where ε'' is fit residua neglected, b_{ij} is the constant coefficient coupled by $S_j(x,y)$ and $Z_j(x,y)$. Because $S_j(x,y)$ and $Z_j(x,y)$ are selected in advance, all b_{ij} can compose a constant coupled metric $B_{M\times N}$.

Then residual wave-front $\phi(x,y)$ in the shaping course can be expressed as:

$$\phi(x,y) = \varphi(x,y) + \omega(x,y) = \sum_{i=1}^{M} e_i Z_i(x,y) , \quad (6)$$

$$e_i = a_i + \sum_{j=1}^{N} b_{ij} v_j . \quad (7)$$

Strehl ratio (SR) is a universal performance evaluation index, and express far field intensity ratio between distortion wave-front and ideal wave-front at light axis. By the orthogonality of Zernike polynomials in unit circle and the principle of physics optics, performance index of residual wave-front J can be simplified as

$$J = SR = \exp(-\sigma_\phi^2) = \exp[-(A_{M\times1} + B_{M\times N}V_{N\times1}) \cdot (A_{M\times1} + B_{M\times N}V_{N\times1})^T] , \quad (8)$$

where σ_ϕ^2 is variance of residual wave-front and $B_{M\times N} = \{b_{ij}\}_{M\times N}$, $V_{N\times1} = \{v_1, v_2 \cdots v_j \cdots v_N\}^T$, $A_{M\times1} = \{a_1, a_2 \cdots a_i \cdots a_M\}^T$. For fixed initial distortion wave-front A and B are two constant metrics, so the expression (8) only depends on V, which accelerates convergence rate of SPGD algorithm.

Besides, expression (8) describes the principle of adaptive optics wave-front shaping and has some theoretical meanings. From above analysis we know that distortion wave-front depends on A and M; deformable mirror depends on N at some conditions; constant coupled metric B depends on M and N. So we can further achieve the relationship between performance index and shaping object, and shaping device can be expressed as

$$J = f(J_0, M, N) , \quad (9)$$

where J_0 is performance index of initial distortion wave-front and reflect distortion degree of initial wave-front at some extent. Expression (9) is more obvious to describe the essence of adaptive optics for wave-front shaping. We next investigate the law of wave-front shaping with SPGD algorithm by selecting different J_0 (by changing A), M and N.

2.2 SPGD algorithm

SPGD algorithm can shape distortion wave-front by controlling actuator voltage of deformable mirror, and the procedure of bilateral SPGD algorithm is as follows[1]:

(1) Produce initial actuator voltage $V^{(0)} =$

$\{v_1^{(0)}, v_2^{(0)} \cdots v_j^{(0)} \cdots v_N^{(0)}\}$, and obtain initial performance index $J^{(0)} = J(V^{(0)})$;

(2) The n-th iterative voltage is $V^{(n)} = \{v_1^{(n)}, v_2^{(n)} \cdots v_j^{(n)} \cdots v_N^{(n)}\}$, and the corresponding performance index is $J^{(n)} = J(V^{(n)})$;

(3) Produce the n-th small random perturbation voltage $\delta V^{(n)} = \{\delta v_1^{(n)}, \delta v_2^{(n)} \cdots \delta v_j^{(n)} \cdots \delta v_N^{(n)}\}$, and the amplitude is $|\delta v_j^{(n)}|_{\max} = \delta$;

(4) Then obtain

$$V_{\pm}^{(n)} = V^{(n)} \pm \delta V^{(n)}, \tag{10}$$

$$\delta J_{\pm}^{(n)} = J(V_{\pm}^{(n)}) - J(V^{(n)}), \tag{11}$$

$$\delta J^{(n)} = \delta J_{+}^{(n)} - \delta J_{-}^{(n)}. \tag{12}$$

(5) Compute $(n+1)$-th iterative voltage is

$$V^{(n+1)} = V^{(n)} + \gamma \delta V^{(n)} \delta J^{(n)}, \tag{13}$$

where γ is gain coefficient;

(6) Make program circulate from (2) to (5) until it satisfies stop condition of program, and iterations n or performance index J can be selected as the stop program.

3 Simulation model

Work principle of wave-front shaping system with SPGD algorithm for adaptive optics[7] shown in Fig. 1 is that performance index J and its variety ΔJ can be computed by performance index analyzer from data collected by CCD, and then the control voltage of deformable mirror $V = v_1, v_2, \cdots\cdots v_N$ is obtained from ΔJ by SPGD algorithm. Circulate this work course according to above procedure until satisfy the stop condition of SPGD algorithm. The essence of system is that the best control voltage of deformable mirror $V_{\text{best}} = \{v_1, v_2 \cdots\cdots v_N\}$ can be gradually found by SPGD algorithm, which makes performance index J gradually approach to 1 and residual wave-front $\phi(x,y)$ gradually become ideal planar wave-front by gradually changing surface function of deformable mirror $w(x,y)$.

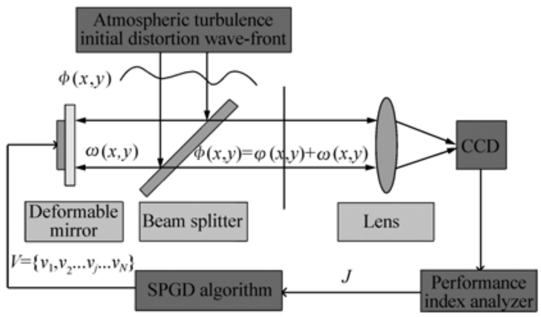

Fig. 1 Wave-front shaping system for with SPGD algorithm for adaptive optics

127, 91, 61, 37, 19, 7[4]-unit deformable mirror were selected as shaping devices and $\omega = 0.08$, $\alpha = 2$ shown in Fig. 2. Atmospheric coherence length $r_o = 13$ cm[10] and caliber of receiving device $D = 1.2$ m were selected, and then 6 frames of distortion wave-front were produced randomly including 3 ~ 119(117) order Zernike aberrations with Roddier method as shaping objects shown in Fig. 3. And $\gamma = 30$, $\delta = 0.1$ and $V^{(0)} = \{0, 0 \cdots 0 \cdots 0\}$ were selected in bilateral SPGD algorithm. Then we use Matlab7. 8. 0 to make simulation experiments respectively for the change law of convergence rate, shaping capability, shaping effect by selecting different combinations among J_0, M and N in computer of Pentium(R) Dual-Core CPU E5300 @ 2. 60 GHz 2. 62 GHz and 32-bit operating system, where J_0 is shown in Fig. 3, $M = 117$, 88, 63, 42, 25, 12, and $N = 127$, 91, 61, 37, 19, 7.

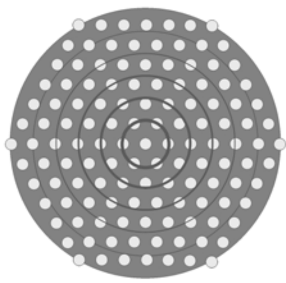

Fig. 2 N-unit deformable mirror (N: 127, 91, 61, 37, 19, 7)

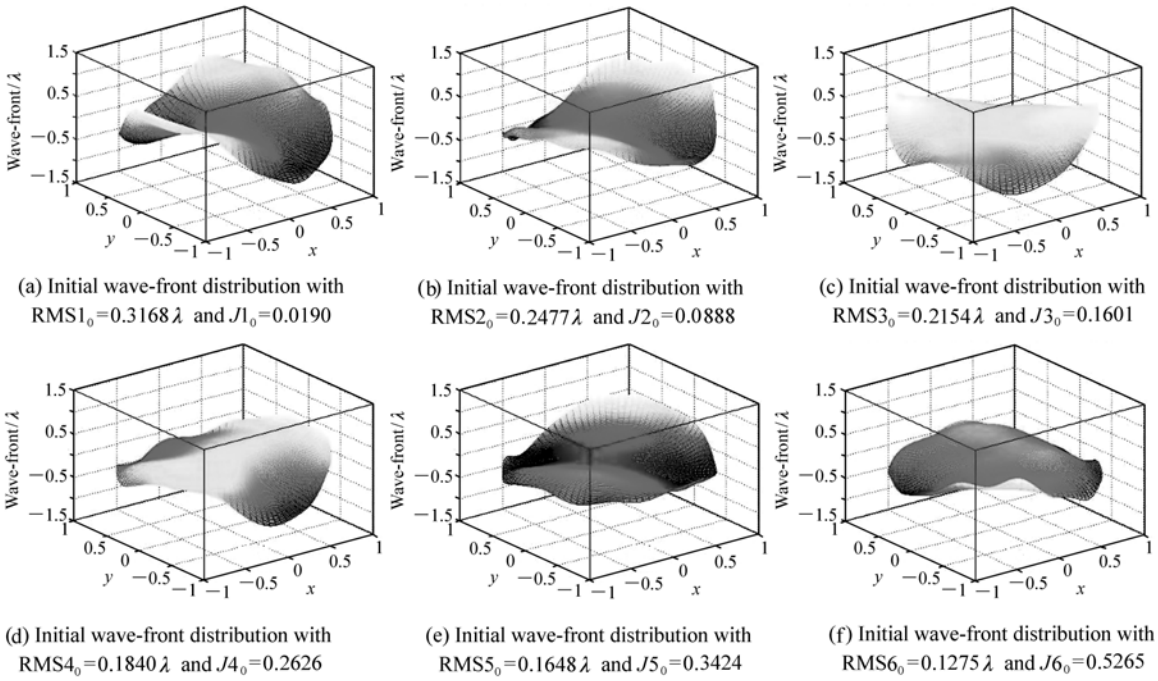

(a) Initial wave-front distribution with $RMS1_0=0.3168\lambda$ and $J1_0=0.0190$

(b) Initial wave-front distribution with $RMS2_0=0.2477\lambda$ and $J2_0=0.0888$

(c) Initial wave-front distribution with $RMS3_0=0.2154\lambda$ and $J3_0=0.1601$

(d) Initial wave-front distribution with $RMS4_0=0.1840\lambda$ and $J4_0=0.2626$

(e) Initial wave-front distribution with $RMS5_0=0.1648\lambda$ and $J5_0=0.3424$

(f) Initial wave-front distribution with $RMS6_0=0.1275\lambda$ and $J6_0=0.5265$

Fig. 3 6 frames of initial distortion wave-front distribution including 3 ~ 119(117) order Zernike aberrations (a: $J1_0=0.0190$, b: $J2_0=0.0888$, c: $J3_0=0.1601$, d: $J4_0=0.2626$, e: $J5_0=0.3424$, f: $J6_0=0.5265$)

4 Simulation results

4.1 Qualitative results of convergence rate of SPGD algorithm

We select iterations $n = 1\,500$ as the stop condition of SPGD algorithm, and achieve 216 sets of convergence curve about the relationship between J and n for different J_0, M and N shown in Fig. 4. A large scale of simulation figures are the same with Fig. 4 in some range of J_0, which mean that convergence course of SPGD algorithm is stable, so selecting randomly a set of results to analyze. We use curve slop dJ/dn to measure convergence rate of SPGD algorithm. Although the local results change, the whole results show that convergence rate increases as Zernike orders M decreases for given J_0 and N, increases as actuator number of deformable mirror N decreases for given J_0 and M, and increases as distortion degree of initial wave-front decreases or J_0 increases for given M and N, where the two latter is more obvious than the former. From expression (8) we can find that the element number MN of coupled constant metric B influences convergence rate, and the fewer MN is, the bigger convergence rate is. So the results are consistent with theoretic analysis. If we use needed iterations up to the same performance index described as n_J or obtained performance index by the same iterations described as J_n to measure convergence rate, achieved conclusions are the same with above conclusions. Besides, it's difficult to obtain quantitative results about convergence rate because it have relations with parameters such as irritations n, voltage amplitude σ, gain coefficient γ and so on[7].

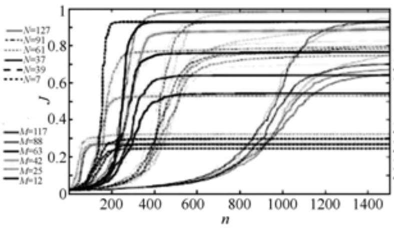

(a) Relationship between J and n with different M and N for $J1_0$=0.0190

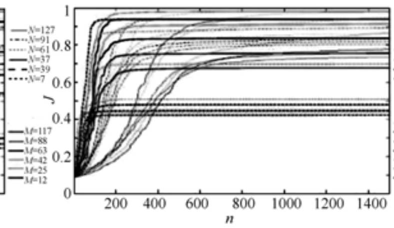

(b) Relationship between J and n with different M and N for $J2_0$=0.0888

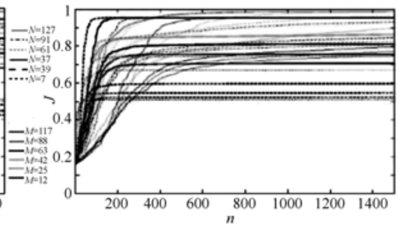

(c) Relationship between J and n with different M and N for $J3_0$=0.1601

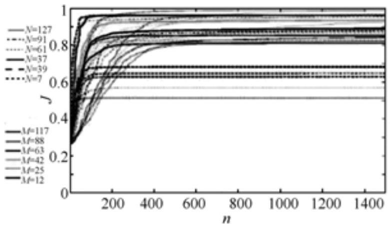

(d) Relationship between J and n with different M and N for $J4_0$=0.2626

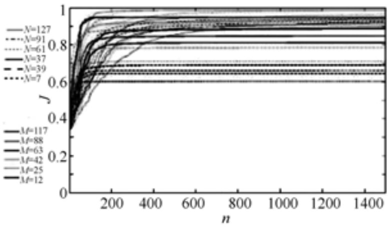

(e) Relationship between J and n with different M and N for $J5_0$=0.3424

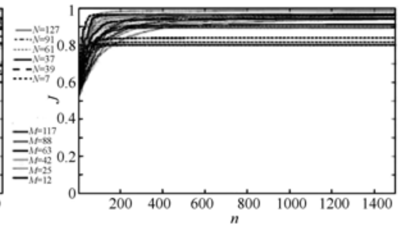

(f) Relationship between J and n with different M and N for $J6_0$=0.5265

Fig. 4 216 sets of convergence curves about the relationship between J and n for different J_0, M and N (a. $J1_0$ = 0.0190, b. $J2_0$ = 0.0888, c. $J3_0$ = 0.1601, d. $J4_0$ = 0.2626, e. $J5_0$ = 0.3424, f. $J6_0$ = 0.5265)

4.2 Qualitative and quantitative results of shaping capability of SPGD algorithm

We can find that every curve will converge to performance index limitation J_{lim}. Here we select irritations n = 5 000 as the stop condition of SPGD algorithm, make $J_{5000} = J_{lim}$ and use J_{lim} to measure shaping capability of SPGD algorithm. Shaping capability J_{lim} for different J_0, M and N are shown in Tab. 1, and corresponding 3 dimension figure are shown in Fig. 5 (a). Although the local results change, the whole results show that shaping capability increases as Zernike orders M decreases when $M \geqslant 25$ and decreases as M decreases when $M \leqslant 25$ for given J_0 and N, increases as actuator number of deformable mirror N decreases when $N \geqslant 91$ and decreases as N decreases when $N \leqslant 91$ for given J_0 and M, and increases as distortion degree of initial wavefront decreases or J_0 increases for given M and N, where the two latter is more obvious than the former. Besides, the results also show that shaping

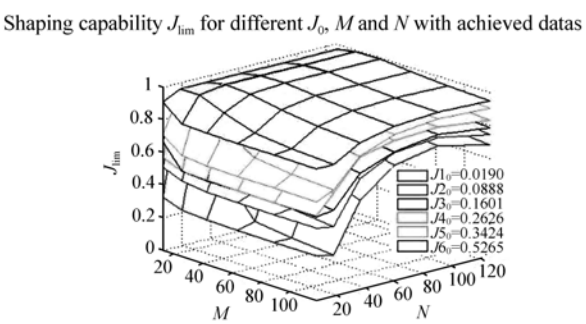

(a) 3d figure with data in Tab.1

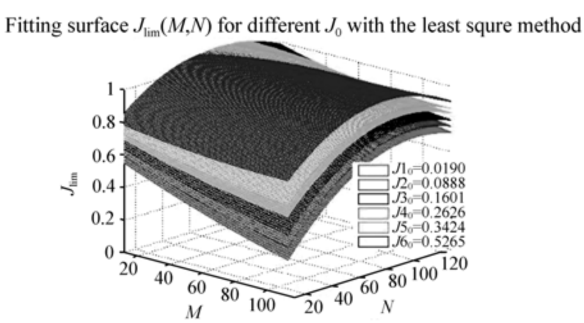

(b) 3d fitting surface with expression (14)

Fig. 5 Shaping capability J_{lim} for different J_0, M and N

capability is the best when $M=42$ and $N=91$. We can achieve quantitative expression (14) of shaping capability about different J_0, M and N with the least square method, and corresponding fitting surfaces for 6 frames of different initial distortion wave-front are shown in figure Fig. 5 (b). Comparisons between Fig. 5 (a) and Fig. 5 (b) indicate that expression (14) can reflect the change law of shaping capability. We can obtain more accurate quantitative expression if we make segment solution or use more data to fit.

$$J_{\lim} = -0.42134274J_0^2 + 0.00000848M^2 - 0.00005865N^2 + 0.00497931J_0M - 0.00486331J_0N + 0.00000661MN + 0.63953653J_0 - 0.00457359M + 0.01108444N + 0.56106810 . \quad (14)$$

Tab. 1　Shaping capability $J_{\lim}$ for different J_0, M and N

$J_{\lim}$	$M \backslash N$	127	91	61	37	19	7
$J1_{\lim}(M,N)$	117	0.680 3	0.754 6	0.702 4	0.543 5	0.245 3	0.268 6
	88	0.702 7	0.780 1	0.761 1	0.641 0	0.266 5	0.268 8
	63	0.743 5	0.802 9	0.835 6	0.766 1	0.297 7	0.269 4
	42	0.965 7	0.989 4	0.963 0	0.903 2	0.531 4	0.270 8
	25	0.984 5	0.984 5	0.984 5	0.984 5	0.806 9	0.285 4
	12	0.929 3	0.929 3	0.929 3	0.929 3	0.929 3	0.323 4
$J2_{\lim}(M,N)$	117	0.746 8	0.807 6	0.783 5	0.676 9	0.422 6	0.438 7
	88	0.774 8	0.825 0	0.821 1	0.755 9	0.447 3	0.439 1
	63	0.810 9	0.848 7	0.867 7	0.838 7	0.479 7	0.439 7
	42	0.979 7	0.991 7	0.968 8	0.926 5	0.698 0	0.444 3
	25	0.982 1	0.982 1	0.982 1	0.982 1	0.898 8	0.462 6
	12	0.939 5	0.939 5	0.939 5	0.939 5	0.939 5	0.508 1
$J3_{\lim}(M,N)$	117	0.787 9	0.824 8	0.787 7	0.706 9	0.521 8	0.509 5
	88	0.804 7	0.843 0	0.810	00.755 0	0.545 2	0.509 9
	63	0.848 2	0.878 4	0.873 5	0.811 9	0.596 3	0.511 0
	42	0.987 2	0.993 3	0.978 7	0.892 7	0.746 9	0.513 1
	25	0.987 1	0.987 1	0.987 1	0.987 1	0.944 4	0.521 0
	12	0.954 3	0.954 3	0.954 3	0.954 3	0.954 3	0.669 5
$J4_{\lim}(M,N)$	117	0.833 0	0.869 2	0.854 7	0.809 9	0.627 6	0.512 0
	88	0.849 1	0.878 3	0.881 6	0.852 8	0.646 3	0.512 1
	63	0.865 3	0.888 3	0.899 7	0.889 3	0.681 8	0.512 1
	42	0.987 9	0.993 4	0.979 5	0.941 5	0.827 0	0.514 8
	25	0.987 3	0.987 3	0.987 3	0.987 3	0.959 5	0.520 8
	12	0.959 7	0.959 7	0.959 7	0.959 7	0.959 7	0.569 8
$J5_{\lim}(M,N)$	117	0.906 1	0.923 0	0.892 8	0.810 6	0.644 4	0.600 8
	88	0.916 3	0.935 1	0.912 7	0.847 3	0.660 4	0.600 9
	63	0.933 0	0.948 9	0.950 5	0.886 6	0.689 5	0.601 1
	42	0.992 6	0.994 7	0.990 4	0.962 1	0.783 6	0.602 9
	25	0.986 7	0.986 7	0.986 7	0.986 7	0.940 8	0.620 9
	12	0.948 0	0.948 0	0.948 0	0.948 0	0.948 0	0.709 0
$J6_{\lim}(M,N)$	117	0.952 2	0.962 8	0.942 4	0.895 9	0.801 1	0.802 2
	88	0.959 1	0.968 6	0.955 0	0.912 1	0.816 3	0.802 6
	63	0.972 8	0.978 8	0.972 9	0.943 3	0.839 4	0.802 7
	42	0.993 9	0.994 6	0.993 1	0.975 6	0.901 8	0.804 3
	25	0.987 7	0.987 7	0.987 7	0.987 7	0.964 1	0.812 5
	12	0.965 4	0.965 4	0.965 4	0.965 4	0.965 4	0.908 9

4.3 Qualitative and quantitative results of shaping effect of SPGD algorithm

We use $\mathrm{RMS}_{\mathrm{lim}}$ to measure shaping effect of SPGD algorithm. Shaping effect $\mathrm{RMS}_{\mathrm{lim}}$ for different J_0, M and N are obtained from expression (15).

$$\mathrm{RMS}_{\mathrm{lim}}=\sqrt{\ln\frac{1}{J_{\mathrm{lim}}}}. \tag{15}$$

Although its change trend is reverse to that of shaping capability, two results are the same and achieved 6 frames of residual wave-front distribution corresponding to 6 frames of different initial distortion wave-front are shown in Fig. 6. Comparisons between Fig. 3(a ~ f) and Fig. 6(a ~ f) indicate SPGD algorithm has good shaping effect.

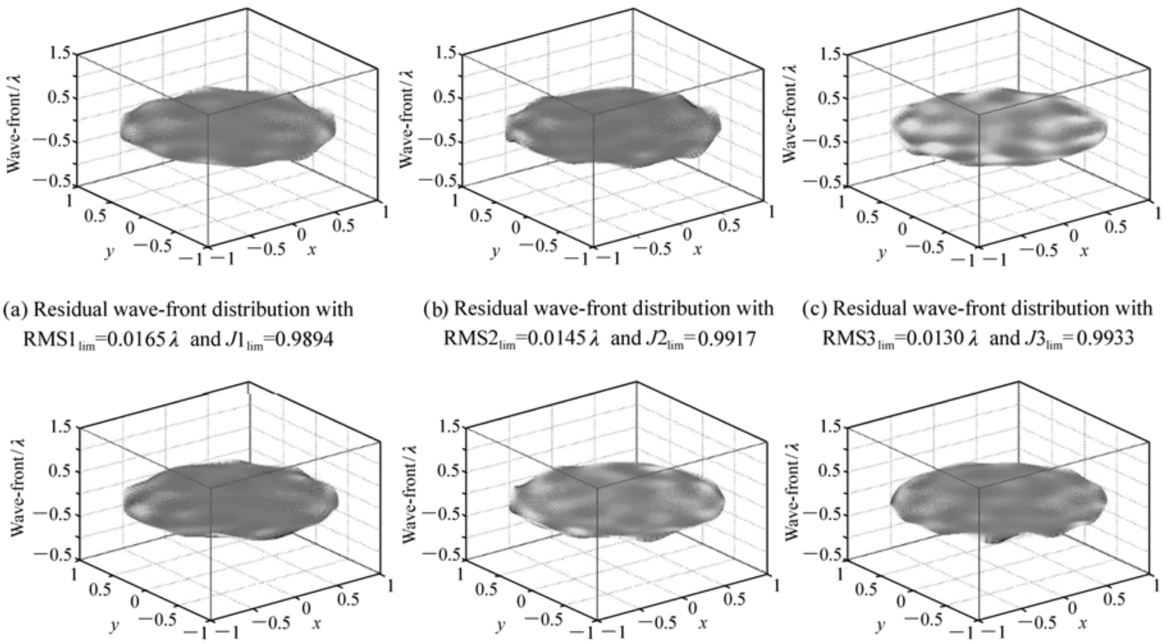

(a) Residual wave-front distribution with $\mathrm{RMS1}_{\mathrm{lim}}=0.0165\lambda$ and $J1_{\mathrm{lim}}=0.9894$

(b) Residual wave-front distribution with $\mathrm{RMS2}_{\mathrm{lim}}=0.0145\lambda$ and $J2_{\mathrm{lim}}=0.9917$

(c) Residual wave-front distribution with $\mathrm{RMS3}_{\mathrm{lim}}=0.0130\lambda$ and $J3_{\mathrm{lim}}=0.9933$

(d) Residual wave-front distribution with $\mathrm{RMS4}_{\mathrm{lim}}=0.0130\lambda$ and $J4_{\mathrm{lim}}=0.9934$

(e) Residual wave-front distribution with $\mathrm{RMS5}_{\mathrm{lim}}=0.0116\lambda$ and $J5_{\mathrm{lim}}=0.9947$

(f) Residual wave-front distribution with $\mathrm{RMS6}_{\mathrm{lim}}=0.0117\lambda$ and $J6_{\mathrm{lim}}=0.9946$

Fig. 6 6 frames of residual wave-front distribution for $M=42$ and $N=91$
(a: $J1_0=0.0190$, b: $J2_0=0.0888$, c: $J3_0=0.1601$, d: $J4_0=0.2626$, e: $J5_0=0.3424$, f: $J6_0=0.5265$)

5 Discussion

We found that shaping capability and shaping effect respectively are difficult to up to $J_{\mathrm{lim}}=1$ or $\mathrm{RMS}_{\mathrm{lim}}=0$. The reason is that deformable mirror don't shape residual high (117-M) order Zernike aberrations corresponding $J_0^{(117\text{-M})}$ and $\mathrm{RMS}_0^{(117\text{-M})}$ shown in Tab. 2, but low M order Zernike aberrations of initial distortion wave-front. Besides, we can find that SPGD algorithm shapes low M order Zernike aberrations wholly when $M\leqslant 25$ and partly when $M\geqslant 25$, which depends on deformable mirror and parameters of SPGD algorithm.

The change laws of convergence rate, shaping capability and shaping effect about distortion degree of initial wave-front, Zernike order and actuator number of deformable mirror are similar, so expression (14) or (15) can analyze qualitatively the law of convergence rate. Besides, we can select the best deformable mirror for different initial distortion wave-front in atmospheric turbulence form expression (14) or (15). Considering the nature of real-time and simplification of adaptive optics it's better to select 37-unit deformable mirror to shape 3 ~ 27(25) order Zernike aberrations at the conditions of some shaping effect.

Tab. 2　$J_0^{(117\text{-}M)}$ and $RMS_0^{(117\text{-}M)}$ of 6 frames of initial distortion wave-front only including (117-M) order Zernike aberrations

M	117	88	63	42	25	12
$J1_0^{(117-M)}$	1.000 0	0.999 1	0.996 9	0.991 0	0.984 5	0.929 3
$J2_0^{(117-M)}$	1.000 0	0.998 7	0.996 1	0.992 4	0.982 1	0.939 5
$J3_0^{(117-M)}$	1.000 0	0.999 0	0.996 7	0.993 6	0.987 1	0.954 3
$J4_0^{(117-M)}$	1.000 0	0.998 8	0.997 2	0.993 8	0.987 3	0.959 7
$J5_0^{(117-M)}$	1.000 0	0.999 3	0.997 8	0.994 8	0.986 7	0.948 0
$J6_0^{(117-M)}$	1.000 0	0.999 5	0.995 8	0.994 6	0.987 7	0.965 4
$RMS1_0^{(117-M)}/\lambda$	0	0.004 8	0.008 8	0.015 1	0.019 9	0.043 1
$RMS2_0^{(117-M)}/\lambda$	0	0.005 7	0.009 9	0.013 9	0.021 4	0.039 8
$RMS3_0^{(117-M)}/\lambda$	0	0.005 0	0.009 2	0.012 7	0.018 1	0.034 4
$RMS4_0^{(117-M)}/\lambda$	0	0.005 4	0.008 4	0.012 6	0.018 0	0.032 3
$RMS5_0^{(117-M)}/\lambda$	0	0.004 3	0.007 5	0.011 5	0.018 4	0.036 8
$RMS6_0^{(117-M)}/\lambda$	0	0.003 7	0.010 4	0.011 7	0.017 7	0.029 9

6　Conclusion

In this paper we mainly make detailed simulations for the laws of convergence rate, shaping capability and shaping effect about distortion wave-front, Zernike order and actuator number of deformable mirror of wave-front shaping system with SPGD algorithm for adaptive optics in atmospheric turbulence. We use 6 kinds of deformable mirror as shaping devices and select 6 frames of distortion wave-front including 3 ~ 119(117) order Zernike aberrations with Roddier method as shaping objects with SPGD algorithm by selecting appropriate parameters to construct simulation model. The qualitative simulation results show that convergence rate increases with the decrease of Zernike order M, actuator number of deformable mirror N, and distortion degree of initial wave-front decreases. Shaping capability and shaping effect have the same terdency, which increase as Zernike orders M decreases when $M \geqslant 25$ and decrease as M decreases when $M \leqslant 25$, increase as actuator number of deformable mirror N decreases when $N \geqslant 91$ and decrease as N decreases when $N \leqslant 91$, and increase as distortion degree of initial wave-front decreases. Shaping capability and shaping effect are the best when $M = 42$ and $N = 91$. And it can be found from discussion that it's better to select 37-unit deformable mirror to shape 3 ~ 27(25) order Zernike aberrations at the conditions of some shaping effect considering the nature of real-time and simplification of adaptive optics system.

参考文献:

[1] WANG S H. Application of stochastic-parallel-gradient-descent adaptive optics techniques in bam cleanup[D]. Changsha: National University of Defense Technology, 2009.

[2] VORONTSOV M A, CARHART G W, RICKLIN J C. Adaptibe phase-distortion correction based on parallel gradient-descent optimization[J]. *Optics Letters*, 1997, 22(12): 907-909.

[3] VORONTSOV M A, GARHART G W, COHEN M, *et al.*. Adaptive optics based on analog parallel stochastic optimization: analysis and experimental demonstration[J]. *J. Opt. Soc. Am. A*, 2000, 17(8): 1440-1453.

[4] VORONTSOV M. Adaptive photonics phase-locked elements (APPLE): system architecture and wavefront control concept

[J]. *SPIE*,2005,5895:1-9.

[5] YANG H Z,LI X Y,GONG C L,*et al*.. Restoration of turbulence-degraded extended object using the stochastic parallel gradient descent algorithm: numerical simulation[J]. *Optics Express*,2009,17(5):3052-3062.

[6] VORONTSOV M A,SIVOKON V P. Stochastic parallel-gradient-descent technique for high-resolution wave-front phase-distortion correction[J]. *J. Opt. Soc. Am. A*,1998,15(10):2745-2757.

[7] YANG H Z,LI X Y,JIANG W H. Simulation and analysis of stochastic parallel gradient descent control algorithm for adaptive optics system[J]. *Acta Optica Sinica*,2007,27(28):1355-1360.

[8] WANG W B,ZHAO S,GUO J,*et al*.. Convergence rate of stochastic parallel gradient descent algorithm based on Zernike mode[J]. *Chinese Optics*,2012,5(4):407-415.

[9] RODDIER N. Atmospheric wavefront simulation using Zernike polynomials[J]. *Optical Engineering*,1990,29(10):1174-1180.

[10] WANG Y R,WANG J Y,XU P,*et al*.. Comparison of experimental analysis of atmospheric coherence length in surface layer[J]. *J. Atmospheric and Environmental Optics*,2010,5(4):263-268.

Author's biography:

WANG Wei-bing(1986—), male, Msc. He received his Msc degree in Changchun institute of optics, fine mechanics and physics, Chinese academy of sciences in 2013, and his research interests mainly focus on adaptive optics for wave-front shaping, control algorithm and electro-optical tracking control technology. E-mail: wangweibing10@126.com

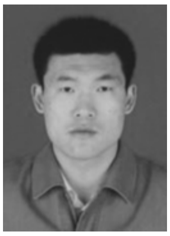

WANG Ting-feng(1977—), male, PhD. He received his PhD degree in Changchun institute of optics, fine mechanics and physics, Chinese academy of sciences in 2005, and his research interests mainly focus on laser application. E-mail: wtfeng@sina.com

GUO Jin(1964—), male, PhD. He received his PhD degree in Changchun institute of optics, fine mechanics and physics, Chinese academy of sciences in 2007, and his research interests mainly focus on laser application. E-mail: guojin1964@126.com